

Enhancement of erbium photoluminescence by substitutional C alloying of Si

M. Markmann, E. Neufeld, A. Sticht, K. Brunner, G. Abstreiter, and Ch. Buchal

Citation: *Appl. Phys. Lett.* **75**, 2584 (1999);

View online: <https://doi.org/10.1063/1.125085>

View Table of Contents: <http://aip.scitation.org/toc/apl/75/17>

Published by the *American Institute of Physics*



SciLight

Sharp, quick summaries **illuminating**
the latest physics research

Sign up for **FREE!**

AIP
Publishing

Enhancement of erbium photoluminescence by substitutional C alloying of Si

M. Markmann,^{a)} E. Neufeld, A. Sticht, K. Brunner, and G. Abstreiter
Walter Schottky Institut, TU München, Am Coulombwall, D-85748 Garching, Germany

Ch. Buchal
ISI 2, Forschungszentrum Jülich GmbH, D-52425 Jülich, Germany

(Received 11 June 1999; accepted for publication 25 August 1999)

Photoluminescence (PL) at 1.54 μm of erbium-doped $\text{Si}_{1-y}\text{C}_y$ alloys grown by molecular beam epitaxy (MBE) has been analyzed depending on sample temperature, excitation density, and growth conditions. Erbium activation raises with increasing incorporation of substitutional carbon compared to interstitial carbon. For $[\text{Er}] = 4.5 \times 10^{19} \text{ cm}^{-3}$ and $y = 0.1\%$ maximum PL output at 1.54 μm was achieved for growth temperatures at 430 °C. Additional annealing could further enhance PL intensity at 1.54 μm . For increasing sample temperature a decrease of PL intensity with two characteristic activation energies around 100 and 10–20 meV is observed, which results in quenching of PL intensity at lower temperatures for Si:Er:C layers compared to Si:Er:O layers. PL spectra show different fine structure for oxygen and carbon codoping by MBE or ion implantation, higher efficiency, and lower PL background for MBE-grown samples in contrast to ion-implanted layers. © 1999 American Institute of Physics. [S0003-6951(99)03043-0]

With silicon being the leading semiconductor material in microelectronics, it is highly desirable to realize silicon-based light emitters for integration of optical components on the same chip. This endeavor has been hampered by the indirect band gap of Si. A possible and promising way to reach this aim is to incorporate erbium in silicon. Erbium ions in their Er^{3+} state exhibit a spectrally sharp transition at the 1.54 μm wavelength. This wavelength coincides with the range of minimal absorption in silicon-based fibers and, therefore, has great commercial importance for optical communication techniques. As is characteristic for rare-earth metals in various host materials, erbium ions can be excited within the 4f shell, resulting in a radiative transition at the desired wavelength. To investigate these optical active layers, different incorporation techniques for erbium and codopants were used, such as ion implantation^{1,2} and molecular beam epitaxy (MBE).^{3,4} Additional codopants, mainly, O, C, and F,^{1–6} play an important role for getting efficient 1.54 μm erbium luminescence up to room temperature: They allow for erbium incorporation in the silicon host up to high concentrations without segregation and enhance luminescence efficiency. So far, oxygen seemed to be the best choice for activating erbium ions enhancing the luminescence output most.⁵ The scope of this work is to analyze the erbium photoluminescence (PL) depending on the carbon incorporation in $\text{Si}_{1-y}\text{C}_y$:Er alloy layers deposited by MBE.

All samples were grown by solid-source MBE. Compared to ion implantation, this technique has the advantage of a high crystal quality, enabling detection of erbium PL in the as-grown state without thermal annealing steps. An 80-nm-thick Si buffer layer and a 200-nm-thick erbium-doped $\text{Si}_{1-y}\text{C}_y$ layer are deposited on an intrinsic (100)Si substrate. The erbium flux is controlled by the temperature of a Knudsen cell. Si is evaporated from an e-beam source at a constant growth rate of 0.3 Å/s. Alloying with carbon was achieved

by sublimation from a current-heated graphite filament. Two-dimensional growth with 2×1 reconstruction was *in situ* controlled by reflection high-energy electron diffraction (RHEED). Secondary ion mass spectroscopy (SIMS) was used to measure the spatial concentration profiles. SIMS data clearly demonstrate that erbium and carbon are incorporated in the concentration range up to 10^{20} cm^{-3} without significant segregation in the active layer. By x-ray diffraction (XRD) spectroscopy in combination with SIMS, we could distinguish between the amounts of carbon on substitutional and interstitial lattice sites. Besides the silicon substrate peak, a well-separated peak originating from the tensile strained $\text{Si}_{1-y}\text{C}_y$ layer as well as pendellösung fringes could be resolved. This indicates a high quality of the layers and interfaces. The PL was excited by the 488 nm line of an Ar^+ -ion laser with an excitation density of about 0.2 W/cm². A single-grating monochromator together with a liquid-nitrogen-cooled germanium detector were used to disperse and detect the PL signal in a lock-in technique.

The integrated PL intensity of the line at 1.54 μm from $\text{Si}_{0.999}\text{C}_{0.001}$:Er layers observed at $T = 7 \text{ K}$ depending on growth temperature is shown in Fig. 1. The Er concentration was $[\text{Er}] = 4.5 \times 10^{19} \text{ cm}^{-3}$. It can be seen that codoping with $y = 0.1\%$ carbon ($[\text{C}] = 3.9 \times 10^{19} \text{ cm}^{-3}$) leads to a strong enhancement of the 1.54 μm luminescence depending on growth temperature. For comparison, a Si:Er sample grown by MBE was implanted with the same amount of carbon. After annealing at 900 °C for 30 min, it showed stronger luminescence compared to samples without carbon codoping, but lower efficiency than the MBE-grown $\text{Si}_{1-y}\text{C}_y$ samples. One can distinguish between two growth temperature ranges with a clear maximum for PL output at 1.54 μm from the Er^{3+} ions for a substrate temperature of about 430 °C: The PL intensity increases with growth temperature up to 430 °C. *In situ* RHEED characterization showed amorphous crystal growth for low temperatures $T < 390 \text{ °C}$. These amorphous layers have a high density of defects and nonra-

^{a)}Corresponding author. Electronic mail: markmann@wsi.tu-muenchen.de

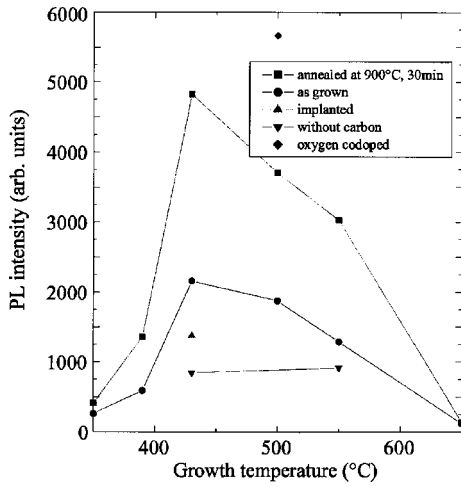


FIG. 1. Integrated PL intensity at 1.54 μm recorded at 7 K as a function of growth temperature for Si:Er samples, codoped with O ($[\text{O}]=3.5 \times 10^{19} \text{ cm}^{-3}$) and C ($[\text{C}]=3.9 \times 10^{19} \text{ cm}^{-3}$), and without any codopant, prepared by MBE or ion implantation.

diative recombination channels causing a short carrier lifetime. This results in less effective excitation of erbium ions in PL measurements via the *impurity Auger effect*.² For growth temperatures higher than 430 °C, the PL output decreases. From combined XRD and SIMS analysis, a reduced substitutional incorporation of carbon is deduced at higher growth temperature. The carbon tends to be incorporated on interstitial lattice sites and may form SiC precipitates and defects like dislocations.⁷ Therefore, excitation of erbium ions shrinks obviously. Annealing at 900 °C for 30 min increases PL efficiency most for all samples (Fig. 1). We observe about the same PL efficiency at 1.54 μm as from our best oxygen codoped 240 nm Si:Er:O layer grown at 500 °C.⁸

PL intensity $I(P_L)$ at 1.54 μm versus excitation power P_L was analyzed for a series of annealing temperatures between 700 and 1100 °C. For all annealing conditions a linear increase in PL intensity followed by a saturation regime can be observed. The power dependence at constant temperature $T=7 \text{ K}$ can be fitted well by a function suggested by Priolo et al.⁵ for Si:Er:O layers:

$$I(P_L) = \frac{A}{1 + B/P_L^n}, \quad A \propto \frac{N^* \tau}{\tau_{tr} \tau_{rad}}, \quad B \propto 1/\tau_{eh},$$

with N^* being the number of excited Er^{3+} ions, τ and τ_{rad} the total and radiative lifetime of the Er^{3+} ions. τ_{tr} is the transit time for filling the excited state of Er^{3+} from the donor level, and τ_{eh} the lifetime of free carriers. The parameter n depends on the recombination mechanism for free carriers and should be between 1 (Shockley–Read–Hall recombination) and 1/3 (additional Auger recombination).⁹ Results of the fit are plotted in Fig. 2: For annealing temperatures up to 900 °C, the saturation PL output at 1.54 μm increases compared to the as-grown state. XRD data indicate no change in substitutional C content in this temperature range. This is attributed to diffusion of carbon on substitutional sites¹⁰ activating further erbium centers. Above 900 °C the substitutional carbon content shrinks (see Fig. 2). Despite the lifetime of the free carrier increases, which should enhance the excitation probability of Er^{3+} , PL intensity also de-

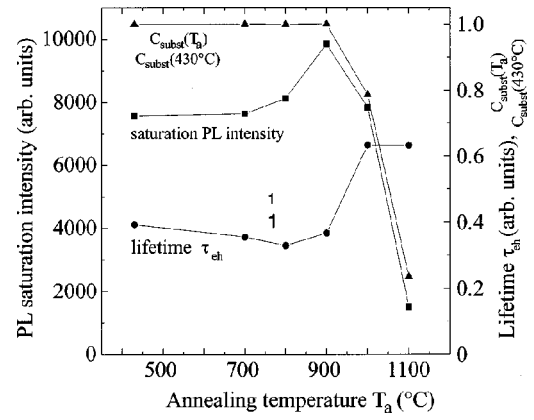


FIG. 2. PL saturation intensity at 1.54 μm , substitutional C fraction, and lifetime τ_{eh} of free carriers vs annealing temperature for a sample with $[\text{Er}]=4.5 \times 10^{19} \text{ cm}^{-3}$ and $[\text{C}]=3.9 \times 10^{19} \text{ cm}^{-3}$ grown at $T_{\text{growth}}=430 \text{ °C}$.

creases. This indicates that activating erbium centers by substitutional carbon incorporation is the crucial point for efficient PL output from $\text{Si}_{1-y}\text{C}_y\text{:Er}$ layers. At constant erbium concentration $4.5 \times 10^{19} \text{ cm}^{-3}$ and growth temperature of 430 °C, the PL intensity at 1.54 μm is increased by raising the total carbon content up to $3.9 \times 10^{19} \text{ cm}^{-3}$. This may be attributed to an improved optical activation by an increased number of carbon atoms surrounding erbium ions or a higher strain caused by substitutional C. Above $[\text{C}]=3.9 \times 10^{19} \text{ cm}^{-3}$, PL decreases strongly. This could be caused by C–C clustering, SiC precipitates, and C-related defects, which enhance nonradiative band-to-band recombination.¹¹

Figure 3 shows typical temperature dependences of the PL output at 1.54 μm from erbium ions. Oxygen and carbon codoped Si:Er layers grown by MBE indicate a similar behavior: Increasing the temperature from 7 to 40 K does not affect the PL intensity I . For higher temperatures, PL output from carbon codoped samples decreases faster compared to Si:Er:O layers. It vanishes at about 170 K while the latter can be observed up to room temperature. For comparison, the implanted Si:Er:C sample shows clear PL only below 90 K. The temperature dependence $I(T)$ can be well approximated by a double-exponential fit⁵ with two activation energies (E_1 and E_2):

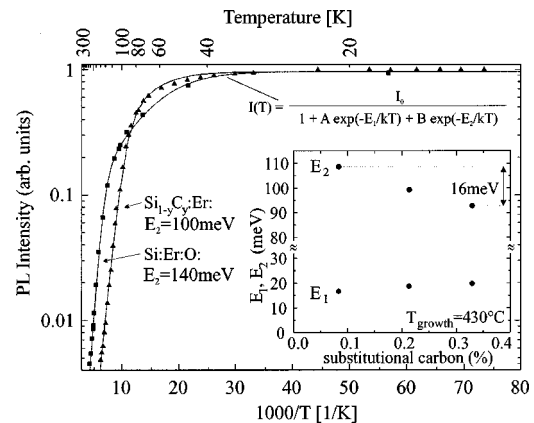


FIG. 3. Typical temperature dependence of the PL intensity at 1.54 μm of erbium-doped $\text{Si}_{1-y}\text{C}_y$ ($[\text{Er}]=4.5 \times 10^{19} \text{ cm}^{-3}$, $y=0.1$, $T_{\text{growth}}=430 \text{ °C}$) and Si:Er:O layers ($[\text{Er}]=[\text{O}]=3.5 \times 10^{19} \text{ cm}^{-3}$, $T_{\text{growth}}=500 \text{ °C}$). Inset: thermal activation energy E_1 and E_2 depending on substitutional carbon content in $\text{Si}_{1-y}\text{C}_y\text{:Er}$ layers grown at $T=430 \text{ °C}$.

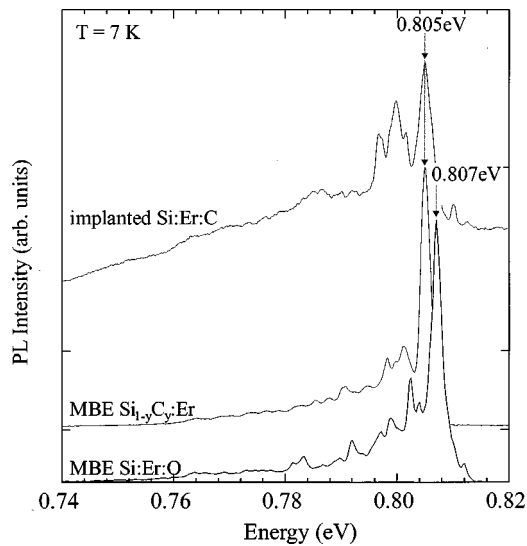


FIG. 4. High-resolution PL spectra at 7 K with spectral resolution of 0.5 meV for MBE-grown oxygen and carbon codoped Si:Er layers as well as an implanted Si_{1-y}C_y:Er sample.

$$I(T) = \frac{I_0}{1 + A \exp(-E_1/kT) + B \exp(-E_2/kT)}.$$

The coupling coefficients are about $A = 20$ and $B = 200\,000$ for all samples. Oxygen codoped erbium ions showed the typical activation energies $E_1 \approx 10$ – 20 meV and $E_2 \approx 140$ meV as already reported.^{5,8} Erbium in Si_{1-y}C_y alloys does not influence significantly the shallow level ($E_1 \approx 10$ – 20 meV), whereas it causes a lower activation energy E_2 . This difference can be seen from the smaller slope of the Si:Er:C data for temperatures above 60 K in Fig. 2. E_2 depends on the substitutional carbon content. Increasing the substitutional carbon content from $y = 0.08\%$ to $y = 0.3\%$, a decrease in activation energy from $E_2 = 108.5$ to 92.8 meV is observed. This change compares well to the band-gap reduction ($\Delta E = -y \cdot 6.5$ eV) of about 16 meV expected for Si_{1-y}C_y alloy layers on Si(100).¹² Tensile biaxial strain in the Si_{1-y}C_y layer causes mainly a decrease of the conduction-band edge, which may imply a conduction-band-related state causing the transition with thermal activation energy E_2 . Finally, it should be mentioned that E_2 in carbon codoped samples has been reported to be 150 meV by Priolo *et al.*⁵ for a significant lower carbon ($c[\text{C}] = 1 \times 10^{18} \text{ cm}^{-3}$) and erbium concentration ($c[\text{Er}] \approx 6 \times 10^{15} \text{ cm}^{-3}$). The discrepancy of the value extrapolated for low y from our data is not understood. It may indicate a different level of Er in Si_{1-y}C_y.

By high-resolution photoluminescence measurements the influence of the local environment on the erbium ion can be studied. Figure 4 shows the PL spectra recorded at 7 K with a spectral resolution of 0.5 meV, normalized to their peak values, of the MBE grown Si:Er:O, MBE-grown and ion-implanted Si:Er:C films. The MBE-grown samples were analyzed in their as-grown state, while the ion-implanted sample was annealed at 900 °C for 30 min. All spectra indicate typical luminescence from erbium. The main peak for oxygen codoping of erbium is centered around 0.807 eV. In contrast, activating erbium with carbon (both by MBE and ion implantation) causes the main peak to occur around 0.805 eV. This is not affected by the background oxygen

concentration (MBE: $[\text{O}] = 1 \times 10^{19} \text{ cm}^{-3}$, ion implantation: $[\text{O}] = 4 \times 10^{18} \text{ cm}^{-3}$), indicating mainly activation of erbium ions by carbon atoms. An obvious difference in fine structure of the PL lines besides the main peak regarding line position and relative intensity can be observed (Fig. 4). This may be caused by different optically active erbium centers for each codopant. Also, incorporation of a codopant on different lattice sites clearly alters the fine structure, as can be deduced from comparing MBE and implanted Si:Er:C layers. This is attributed to an increased substitutional content for MBE samples in contrast to mainly interstitial carbon in implanted Si:Er:C layers. This changes the local field around Er³⁺ ions, which results in different Stark splitting of the erbium levels. The sample implanted with carbon reveals intensive background PL and lower PL intensity at $1.54 \mu\text{m}$ than the MBE samples. This could be attributed to implantation-related defects and, therefore, reduced erbium excitation.

We have presented a study on the influence of codopant carbon in MBE-grown Si_{1-y}C_y:Er layers on erbium PL emission at $1.54 \mu\text{m}$. At a carbon concentration of $3.9 \times 10^{19} \text{ cm}^{-3}$ and an erbium concentration of $4.5 \times 10^{19} \text{ cm}^{-3}$, maximum PL output can be achieved for the growth temperature of about 430 °C. Annealing further increases the PL intensity by a factor up to 3 due to a better Er³⁺ activation by substitutional carbon. These Si_{1-y}C_y:Er layers show about the same PL efficiency as the oxygen codoped samples. The temperature dependence of the PL intensity from the Si_{1-y}C_y:Er layers can be described by a double-exponential fit. The activation energy E_2 decreases for higher carbon content on substitutional lattice sites. The PL fine structure for oxygen and carbon codoped samples is different due to a different local environment of the erbium ions. Compared to implanted samples, MBE-grown Si_{1-y}C_y:Er layers show higher PL efficiency, improved T quenching, as well as lower defect-induced background PL.

The samples were grown in a converted Riber MBE system which was provided by H. Kurz of RWTH Aachen, Germany. This project is supported financially by the Volkswagen Stiftung via Photonik. One of the authors (M.M.) gratefully acknowledges financial support from the Studienstiftung des deutschen Volkes.

¹B. Zheng, J. Michel, F. Y. G. Ren, L. C. Kimerling, D. C. Jacobson, and J. M. Poate, Appl. Phys. Lett. **64**, 2842 (1994).

²F. Priolo, G. Franzò, S. Coffa, and A. Carnera, Phys. Rev. B **57**, 4443 (1998).

³E. Neufeld, A. Sticht, A. Luigart, K. Brunner, and G. Abstreiter, Appl. Phys. Lett. **73**, 3061 (1998).

⁴J. Stimmer, A. Reittinger, J. F. Nützel, G. Abstreiter, H. Holzbrecher, and Ch. Buchal, Appl. Phys. Lett. **68**, 3290 (1996).

⁵F. Priolo, G. Franzò, S. Coffa, A. Polman, S. Libertino, R. Barklie, and D. Carey, J. Appl. Phys. **78**, 3874 (1995).

⁶F. Priolo, S. Coffa, G. Franzò, C. Spinella, A. Carnera, and V. Bellani, J. Appl. Phys. **74**, 4936 (1996).

⁷M. W. Dashiell, L. V. Kulik, D. Hits, J. Kolodzey, and G. Watson, Appl. Phys. Lett. **72**, 833 (1998).

⁸E. Neufeld, A. Sticht, K. Brunner, G. Abstreiter, H. Holzbrecher, H. Bay, and Ch. Buchal, Appl. Phys. Lett. **71**, 3129 (1997).

⁹A. Schenk and W. Fichtner, Technical Report No. 92/22, ETH Zürich.

¹⁰C. Penn, S. Zerlauth, J. Stangl, G. Bauer, G. Brunthaler, and F. Schäffler, J. Vac. Sci. Technol. B **16**, 1713 (1998).

¹¹G. G. Fischer, P. Zaumseil, E. Bugiel, and H. J. Osten, J. Appl. Phys. **77**, 1934 (1995).

¹²K. Brunner, K. Eberl, and W. Winter, Phys. Rev. Lett. **76**, 303 (1996).